RSC Advances

PAPER

View Article Online
View Journal | View Issue

Open Access Article. Published on 24 March 2021. Downloaded on 11/15/2025 10:46:23 AM.
This article is licensed under a Creative Commons Attribution-NonCommercial 3.0 Unported Licence.

Check for updates

Cite this: *RSC Adv.*, 2021, **11**, 12066

Two models to estimate the density of organic cocrystals†

Jun-Hong Zhou,*[a] Li Zhao,[b] Liang-Wei Shi[c] and Pei-Cheng Luo*[b]

Received 4th December 2020
Accepted 8th March 2021

DOI: 10.1039/d0ra10241e

rsc.li/rsc-advances

Two models for predicting the density of organic cocrystals composed of energetic organic cocrystals and general organic cocrystals containing nitro groups were obtained. Sixty organic cocrystals in which the ratio of component molecules is 1 : 1 were studied as the dataset. Model-I was based on the artificial neural network (ANN) to predict the density of the cocrystals, which used (six) input parameters of the component molecules. The root mean square error (RMSE) of the ANN model was 0.033, the mean absolute error (MAE) was 0.023, and the coefficient of determination (R^2) was 0.920. Model-II used the surface electrostatic potential correction method to predict the cocrystal density. The corresponding RMSE, MAE, and R^2 were 0.055, 0.045, and 0.716, respectively. The performance of Model-I is better than that of Model-II.

1 Introduction

Nowadays, with the development of modern national defense and military industry, research on energetic materials (EMs) has attracted considerable attention. Pure crystals of EMs could not meet the needs of today's military development; therefore, numerous researchers have put their hearts into the study of energetic cocrystals (ECCs). ECCs are built by combining an energetic molecule with one or more molecules through non-covalent interactions in the same lattice. ECCs show great performance with high energy and low sensitivity compared with pure EMs.

For example, Yang[1] has prepared a 1 : 1 cocrystal explosive by combining 2,4,6,8,10,12-hexanitrohexaazaisowurtzitane (CL-20) and benzotrifuroxan (BTF), and the cocrystal exhibits excellent performance compared with the pure components. Bolton[2] *et al.* have discovered and characterized an ECC, which is composed of CL-20 and 2,4,6-trinitrotoluene (TNT) at a molar ratio of 1 : 1. This cocrystal combines the economic and stability factors of TNT with the density and power of CL-20 into a homogenous energetic compound with high explosive power and excellent insensitivity. Xue[3] *et al.* have found that the cocrystal of CL-20/HMX can mediate the thermal stability of the pure crystal. Zhang and Guo[4] have discovered and characterized five novel 1 : 1 molar ratio cocrystals, which were composed of BTF and a variety of energetic materials. They found that not all cocrystals exhibited excellent performance in comparison with pure BTF.

The solid-state density of the energetic material is the primary physical factor in detonation performance. The energy is usually characterized by detonation velocity and pressure, which are proportional to the density according to the Kamlet–Jacobs equations.[5] For ECC research, the high density cocrystals are our research goal. The loading density of a cocrystal explosive is determined by chemical composition, crystal packing, and intermolecular binding strength. However, the relationship between the cocrystal density and the pure component density is uncertain. Kira *et al.*[6] have researched 17 cocrystals of the benchmark energetic material, TNT, and many of these cocrystals have a density in between those of both components. However, this is not always the case, and some cocrystals have a density higher than those of two pure crystals. Therefore, it is important to choose the appropriate compound to get the cocrystal that has a high density. Nowadays, numerous researchers have obtained cocrystals with some excellent properties by numerous experimental attempts and it is time consuming and dangerous. So, it is urgent to find an accurate model to predict the cocrystal density before the experimental operation.

Zhang[7] *et al.* have supplied a method (eqn (1)) for calculating the cocrystal density, and they supposed that the systems are composed of mixtures of pure components. m_i is the mass of component i, and $d_{298K,i}$ is the density of component i.

$$d_{mix} = \frac{\sum m_i}{\sum m_i / d_{298\ K,i}} \quad (1)$$

This equation only supplied a rough calculation of the cocrystal density. Strictly speaking, the density of the mixture of pure components is different from that of the cocrystal of pure

[a]Department of Computer Chemistry and Cheminformatics, Shanghai Institute of Organic Chemistry, Chinese Academy of Sciences, 345 LingLing Road, Shanghai, 200032, China. E-mail: zhoujh8@sioc.ac.cn

[b]School of Chemistry & Chemical Engineering, Southeast University, 211189 Nanjing, China. E-mail: luopeicheng@seu.edu.cn

[c]CAS Key Laboratory of Energy Regulation Materials, Chinese Academy of Sciences, 345 LingLing Road, Shanghai, 200032, China

† Electronic supplementary information (ESI) available. See DOI: 10.1039/d0ra10241e

© 2021 The Author(s). Published by the Royal Society of Chemistry

Open Access Article. Published on 24 March 2021. Downloaded on 11/15/2025 10:46:23 AM.
This article is licensed under a Creative Commons Attribution-NonCommercial 3.0 Unported Licence.

components because the mixture density does not consider the intermolecular interactions between the pure components.

Fathollahi *et al.*[8] have built models for predicting the densities of the energetic cocrystals using artificial neural network and multiple linear regression (MLR) based on three dragon descriptors (Ms, Elu, and RTm). In their study, while building the model, a cocrystal descriptor is denoted by CD (eqn (2)), and R_1 and R_2 are the mole fractions of the first and second components, respectively. D_1 and D_2 are the descriptors of the first and second components, respectively.

$$\mathrm{CD} = (R_1 \times D_1) + (R_2 \times D_2) \tag{2}$$

The correlation coefficient (R^2) of the ANN and MLR models (for the whole dataset) was 0.9716 and 0.9309, respectively. The average absolute relative deviation of the ANN model for the complete dataset was 2.48%.

Zohari[9] has researched the relationship between the densities of energetic cocrystals through a quantitative structure–property relationship (QSPR) model (eqn (3)).

$$\rho = 1913 + 0.017\mathrm{sp} + 0.003\mathrm{OB} + 0.008\mathrm{DU} - 0.0128n_{\mathrm{AT}} + 0.136\rho^{+} \tag{3}$$

where ρ is the density of the compound in g cm^{-3}, sp is the sum of the atomic polarizabilities, OB is the value of the oxygen balance, DU is the degree of unsaturation of the compound, n_{AT} is the number of atoms, and ρ^{+} is a correction factor. The research methodology provides a new model that can relate the density of an energetic co-crystal to several molecular structural descriptors, which are calculated by the Dragon[10] software. Dragon is a well-known software that can supply the calculation of more than 1600 molecular descriptors from several input formats (MDL, SYBYL, HyperChem, and Smiles). The determination coefficient (R^2) of the derived correlation was 0.937.

Krishna *et al.*[11] have developed a model for predicting the density of cocrystals using artificial neural network based on some descriptors, such as mass weight, binding energy, melting point, and pK_a.

In these existing models about the prediction of the density of the energetic cocrystals, most models did not consider the interactions between the two components of the cocrystals, so these models are not accurate enough to predict the density of the energetic cocrystals. In the present study, to predict the density of the energetic cocrystal, we chose the energetic organic cocrystals that have been synthesized as the main research objects. To increase the dataset and enhance the credibility of the model, some general organic cocrystals, which contain nitro groups and whose densities are higher than 1.4 g cm^{-3} and the ratio of whose components is 1 : 1, were also selected as the dataset.

The two models to predict the densities of ECCs were built. For Model-I, we used the ANN model to predict the density of the organic cocrystal that uses three input parameters as the factors affecting the density of the organic cocrystal. For Model-II, we have used the Politzer[12,13] method, which was based on the molecular surface electrostatic potential (MESP) to predict the energetic cocrystal density. The method based on MESP has always been used to predict the density of the pure energetic compound. In the present study, we tried to predict the density of the cocrystal. In order to compare the prediction results with those of Model-I, the same dataset as Model-I was used as the research object.

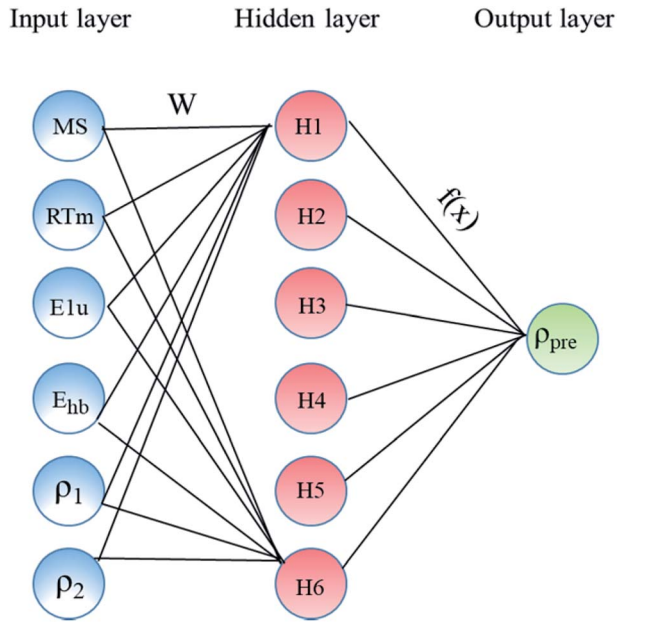

Fig. 1 Architecture of the constructed ANN model consists of three main layers: input, hidden, and output layers.

2 Methods and calculations

In the present study, our major objective is to look for suitable expression parameters, so directly referring to the ref. 11, the ANN was selected as the machine learning algorithm. The ANN model was built as shown in Fig. 1, which includes an input layer, a hidden layer, weights, a sum function, an activation function, and an output layer. The input layer acts as the training sample, and the number of nodes in the input layer is the sample size.

The hidden layer is the operation black box used for connecting the input layer and output layer, and the number of nodes and number of layers can be customized. The output layer is the calculation result, which is mainly used for different calculations

Table 1 The network parameters in the MATLAB toolbox

Topology	6 inputs, 1 output, and 1 hidden layer with 3 neurons (6 × 3 × 1)
Data	Training set: 42 randomly selected cocrystals Test set: 9 randomly selected cocrystals Validation set: 9 randomly selected cocrystals
Beginning function	log-sigmoid
Training algorithm	Levenberg–Marquardt
Loss function conditions	Minimum MSE
Stopping condition	The network stops in one of three ways: validation check > 10, minimum gradient < 10^{-7}, momentum speed > 10^{10}

Open Access Article. Published on 24 March 2021. Downloaded on 11/15/2025 10:46:23 AM.
This article is licensed under a Creative Commons Attribution-NonCommercial 3.0 Unported Licence.

Table 2 The prediction results of the 60 organic cocrystals using artificial neural network models (g cm^{-3} for the density units)

No.	Co-formers	Ref. code	ρ_{exp}	ρ_{ANN}	Re%
Training dataset					
1	CL-20:TNT	IZUZUZ	1.911	1.930	0.994
2	CL-20:AZ2	TETTAQ	1.939	1.938	−0.052
3	CL-20:NEX-1	WEPGEG	1.882	1.874	−0.425
4	CL-2:TODAAZ	HIVGAW	1.971	1.958	−0.660
5	CL-20:BQN	ROSMOD	1.737	1.745	0.461
6	CL-20:DNB	TIVJUF	1.880	1.881	0.053
7	CL-20:4,5-MDNI	NILCIX	1.882	1.877	−0.266
8	HMX:PNO	WEPTAP	1.700	1.697	−0.176
9	HMX:FA	ZEZHET	1.687	1.687	0
10	BTF:TNA	ZEVNUL	1.811	1.819	0.442
11	BTF:MATNB	GEXMON	1.804	1.814	0.554
12	BTF:TNA	GEXMIH	1.884	1.867	−0.902
13	TNT:NNAP	TOZMUS	1.539	1.565	1.689
14	TNT:1-BN	URIJAH	1.737	1.698	−2.245
15	TNT:Ant	URIJEL	1.515	1.532	1.122
16	TNT:9-BN	URIJIP	1.688	1.715	1.600
17	TNT:Per	URIJUB	1.531	1.536	0.327
18	TNT:T2	URIKEM	1.677	1.675	−0.119
19	TNT:DMB	URILEN	1.501	1.508	0.466
20	ABA:TNT	URILUD	1.594	1.589	−0.314
21	MACIC:TZM	ACERAD	1.605	1.623	1.121
22	MBD:MTNB	DIFZOK	1.522	1.480	−2.760
23	PM:UREA	EFOZAB03	1.644	1.648	0.243
24	MC:PC	FIXROV01	1.606	1.661	3.425
25	NDT:THTZT	FOYSUJ	1.664	1.657	−0.421
26	IDT:NTZ	FUFSOQ	1.644	1.651	0.426
27	DNBA:BA	GAUTAM15	1.697	1.655	−2.475
28	PZ:OA	GUDSUV	1.609	1.627	1.119
29	TNP:MDNI	HARJOB	1.769	1.768	−0.057
30	NF:CA	LEWTAK	1.627	1.627	0
31	NF:UREA	ORUXUV	1.661	1.652	−0.542
32	NPO:PA	OWIYEZ	1.682	1.653	−1.724
33	UREA:CA	PANVUV	1.672	1.654	−1.077
34	PZCX:DHXBED	PAQNOM	1.628	1.608	−1.229
35	DNPA:ODADA	QARQUY	1.775	1.772	−0.169
36	TNP:TAD	QONYUP	1.685	1.655	−1.780
37	IZO:DLTA	RUWPEG	1.656	1.648	−0.483
38	IZO:LTA	UHACIQ	1.631	1.646	0.920
39	IZO:LTA	UHAFEP	1.607	1.616	0.560
40	DNBZA:TZ	UNAWUD	1.640	1.655	0.915
41	TZTM:HP	YAFFUJ	1.636	1.635	−0.061
42	BM:TNP	YUQHEY	1.616	1.663	2.908
Test dataset					
43	CL-20:MTNP	QAPNAZ	1.932	1.928	−0.207
44	CL-20:GTA	XAQFUS	1.650	1.571	−4.788
45	CL-20:NFQN	ROSMIX	1.774	1.659	−6.483
46	DHDS:TZM	ACETEJ	1.625	1.655	1.846
47	AB:MTNB	FONHOH	1.442	1.513	4.924
48	DNBA:TA	IJAKAH	1.635	1.655	1.223
49	NMI:NMI	ITIXUE	1.660	1.657	−0.181
50	AN:HP	JOZZED	1.614	1.647	2.045
51	Urea:OA	UROXAM	1.679	1.605	−4.407
Validation dataset					
52	CL-20:DNG	JABYOD	1.750	1.770	1.143
53	HMX:PDCA	ZEZGOC	1.630	1.658	1.718
54	BTF:TNB	GEXMED	1.806	1.838	1.772
55	TNT:DMDBT	URIKUC	1.496	1.523	1.805
56	TNT:PDA	URILAJ	1.578	1.561	−1.077
57	TNT:TNB	NIBJUF	1.640	1.653	0.793
58	DNBZA:NA	AWUDEB	1.607	1.671	3.983
59	PZCX:OA	UZODUK	1.628	1.651	1.413
60	TZA:NDTZI	VAZBIJ	1.790	1.698	−5.140

with the expected output. Through error feedback, the weights between the nodes of the hidden layer are adjusted, and then the new result is the output. The error feedback is repeated until the error is within the allowed range. Table 1 lists the main parameters used in the ANN model using the MATLAB toolbox. This includes network topology, training algorithm, and the number of data points of each dataset (training, test, and validation). In the present study, only one hidden layer network was chosen because the number of the samples is only 60, and it is too few.

The names of the components of the 60 organic cocrystals are listed in Table S1 (see ESI).† The three input parameters of the 60 organic cocrystals, that is, the densities of the two components that make up the cocrystals, ρ_1 and ρ_2, the strongest hydrogen bond interaction (E_{hb}), and the three dragon descriptors (Ms, RTm, and E1u)[8] are listed in Table S2 (see ESI).† The strongest hydrogen bond interaction (E_{hb}) can be calculated using the following formula.[14,15]

$$\alpha_{max} = 0.0000162 \times MEP_{max}{}^2 + 0.00962 \times MEP_{max} \quad (4)$$

$$\beta_{max} = 0.000146 \times MEP_{min}{}^2 - 0.00930MEP_{min} \quad (5)$$

$$E_{max} = -\alpha_{max}\,\beta_{max} \quad (6)$$

where MEP_{max} and MEP_{min} are the maximum and minimum values on the map of electrostatic potential surface (MEPS) of the gaseous molecule. α_{max} and β_{max} are the parameters of the strongest hydrogen bond donor and acceptor, respectively. Suppose that the cocrystal A_mB_n is formed by the compounds A and B.

$$E_{(max,A)} = -\alpha_{(max,A)}\beta_{(max,A)} \quad (7)$$

$$E_{(max,B)} = -\alpha_{(max,B)}\beta_{(max,B)} \quad (8)$$

$$E_{(max,AB1)} = -\alpha_{(max,A)}\beta_{(max,B)} \quad (9)$$

$$E_{(max,AB2)} = -\alpha_{(max,B)}\beta_{(max,A)} \quad (10)$$

and

$$E_{(max,AB)} = \min(E_{(max,AB1)}, E_{(max,AB2)}) \quad (11)$$

$$\Delta E_A = E_{(max,AB)} - E_{(max,A)} \quad (12)$$

$$\Delta E_B = E_{(max,AB)} - E_{(max,B)} \quad (13)$$

and

$$\Delta E_{hb} = \min(\Delta E_A, \Delta E_B) \quad (14)$$

 © 2021 The Author(s). Published by the Royal Society of Chemistry

Open Access Article. Published on 24 March 2021. Downloaded on 11/15/2025 10:46:23 AM.
This article is licensed under a Creative Commons Attribution-NonCommercial 3.0 Unported Licence.

Table 3 Prediction results of the 60 organic cocrystals using surface electrostatic potential correction models (g cm^{-3} for the density unit)

	Co-formers	Ref. code	ρ_{exp}	ρ_P	Re%
1	CL-20:TNT	IZUZUZ	1.911	1.853	−3.023
2	CL-20:DNG	JABYOD	1.750	1.811	3.464
3	CL-20:MTNP	QAPNAZ	1.932	1.882	−2.574
4	CL-20:AZ2	TETTAQ	1.939	1.877	−3.213
5	CL-20:NEX-1	WEPGEG	1.882	1.898	0.837
6	CL-20:GTA	XAQFUS	1.650	1.749	6.010
7	CL-2:TODAAZ	HIVGAW	1.971	1.878	−4.721
8	CL-20:NFQN	ROSMIX	1.774	1.812	2.155
9	CL_20:BQN	ROSMOD	1.737	1.839	5.864
10	CL-20:DNB	TIVJUF	1.880	1.860	−1.070
11	CL-20:4,5-MDNI	NILCIX	1.882	1.849	−1.770
12	HMX:PNO	WEPTAP	1.700	1.698	−0.094
13	HMX:FA	ZEZHET	1.687	1.741	3.205
14	HMX:PDCA	ZEZGOC	1.630	1.698	4.164
15	BTF:TNA	ZEVNUL	1.811	1.876	3.612
16	BTF:TNB	GEXMED	1.806	1.823	0.940
17	BTF:MATNB	GEXMON	1.804	1.807	0.178
18	BTF:TNA	GEXMIH	1.884	1.820	−3.414
19	TNT:NNAP	TOZMUS	1.539	1.627	5.740
20	TNT:1-BN	URIJAH	1.737	1.740	0.151
21	TNT:Ant	URIJEL	1.515	1.565	3.305
22	TNT:9-BN	URIJIP	1.688	1.712	1.404
23	TNT:Per	URIJUB	1.531	1.540	0.616
24	TNT:T2	URIKEM	1.677	1.556	−7.213
25	TNT:DMDBT	URIKUC	1.496	1.544	3.187
26	TNT:PDA	URILAJ	1.578	1.623	2.882
27	TNT:DMB	URILEN	1.501	1.585	5.585
28	TNT:TNB	NIBJUF	1.640	1.744	6.364
29	ABA:TNT	URILUD	1.594	1.636	2.632
30	MACIC:TZM	ACERAD	1.605	1.621	1.027
31	DHDS:TZM	ACETEJ	1.625	1.667	2.555
32	DNBZA:NA	AWUDEB	1.607	1.633	1.648
33	MBD:MTNB	DIFZOK	1.522	1.589	4.434
34	PM:UREA	EFOZAB03	1.644	1.574	−4.243
35	MC:PC	FIXROV01	1.606	1.614	0.470
36	AB:MTNB	FONHOH	1.442	1.509	4.618
37	NDT:THTZT	FOYSUJ	1.664	1.685	1.237
38	IDT:NTZ	FUFSOQ	1.644	1.676	1.931
39	DNBA:BA	GAUTAM15	1.697	1.555	−8.347
40	PZ:OA	GUDSUV	1.609	1.577	−1.977
41	TNP:MDNI	HARJOB	1.769	1.745	−1.367
42	DNBA:TA	IJAKAH	1.635	1.679	2.712
43	NMI:NMI	ITIXUE	1.660	1.668	0.504
44	AN:HP	JOZZED	1.614	1.579	−2.151
45	NF:CA	LEWTAK	1.627	1.670	2.634
46	NF:UREA	ORUXUV	1.661	1.689	1.673
47	NPO:PA	OWIYEZ	1.682	1.729	2.806
48	UREA:CA	PANVUV	1.672	1.680	0.477
49	PZCX:DHXBED	PAQNOM	1.628	1.649	1.302
50	DNPA:ODADA	QARQUY	1.775	1.708	−3.761
51	TNP:TAD	QONYUP	1.685	1.652	−1.930
52	IZO:DLTA	RUWPEG	1.656	1.645	−0.686
53	IZO:LTA	UHACIQ	1.631	1.617	−0.873
54	IZO:LTA	UHAFEP	1.607	1.630	1.420
55	DNBZA:TZ	UNAWUD	1.640	1.689	3.015
56	Urea:OA	UROXAM	1.679	1.691	0.707
57	PZCX:OA	UZODUK	1.628	1.613	−0.942
58	TZA:NDTZI	VAZBIJ	1.790	1.705	−4.740
59	TZTM:HP	YAFFUJ	1.636	1.562	−4.515
60	BM:TNP	YUQHEY	1.632	1.649	1.028

where $E_{(max,A)}$ and $E_{(max,B)}$ denote the pairing energies of the strongest hydrogen bond between A–A and B–B in the pure crystal of compounds A and B. $E_{(max,AB)}$ denotes those in cocrystal A_mB_n. ΔE_{max} denotes the energy difference. The higher the $-\Delta E_{max}$, the more probable is the formation of the cocrystal. $-\Delta E_{max}$ is taken as the criterion to indicate the possibility of cocrystal formation. The method based on the above description can be called the strongest intermolecular site pairing energy method (SISPE). The corresponding computations were implemented in multiwfn3.6.[16] The program multiwfn can realize the electronic wavefunction analysis.

Normalization is to facilitate the rapid learning of neural networks and grasp the logical relationship between the data. Therefore, before performing the artificial neural network calculation, all inputs (descriptors values) were normalized between −1 and +1 using the following equation:

$$A_i = \frac{x_i - x_{min}}{x_{max} - x_{min}} \times (r_{max} + r_{min}) + r_{min} \tag{15}$$

where x_i is the input or output of the model, A_i is the normalized value of x_i, x_{min} and x_{max} are the minimum and maximum values of x_i, respectively, and r_{min} and r_{max} describe the limits of the range where x_i should be scaled.

Model-II is based on the surface electrostatic potential correction method. The following eqn (16) reflects the features of the molecules' surface electrostatic potentials.

$$\text{Cocrystal density} = \alpha\left(\frac{M}{V_m}\right) + \beta\left(\upsilon\sigma_{tot}{}^2\right) + \gamma \tag{16}$$

where M is the molecular mass and V_m is the volume of the isolated gas phase molecule that is enclosed by the 0.001 au contour of its electronic density. The $\upsilon\sigma_{tot}{}^2$ reflects the features of the molecules' surface electrostatic potentials. The two parameter values of V_m and $\upsilon\sigma_{tot}{}^2$ can be computed using the Multiwfn software, and the value of M can be calculated according to the cocrystal molecular formula. The calculation values of M, V_m, and $\upsilon\sigma_{tot}{}^2$ for the 60 cocrystals are listed in Table S3 (see ESI).†

In order to assess the prediction results of the artificial neural network model and the surface electrostatic potential correction model, the relative percentage error (Re%) of the 60 cocrystal samples in the artificial neural network model and the surface electrostatic potential correction model were calculated, respectively. The RMSE, MAE, and R^2 of the artificial neural network model and the surface electrostatic potential correction model were also calculated. The specific calculation of Re%, RMSE, MAE, and R^2 are showed in the following formula.

$$\text{Re\%} = \frac{y_{pre} - y_{exp}}{y_{exp}} \times 100\% \tag{17}$$

$$\text{RMSE} = \sqrt{\frac{\sum_{i=1}^{n}\left(y_{pre} - y_{exp}\right)^2}{N}} \tag{18}$$

$$\text{MAE} = \frac{1}{N}\sum_{i=1}^{n}\left|y_{pre,i} - y_{exp,i}\right| \tag{19}$$

Open Access Article. Published on 24 March 2021. Downloaded on 11/15/2025 10:46:23 AM.
This article is licensed under a Creative Commons Attribution-NonCommercial 3.0 Unported Licence.

Table 4 Parameters and the predicted density of the 6 optimized cocrystals[a]

Co-formers	Ref. code	M	V_m	M/V_m	$\upsilon\sigma_{tot}^2$	ρ_{exp}	ρ_{pre}	Re%
CL-20:AZ2	TETTAQ	672.320	498.763	1.348	42.282	1.939	1.992	2.733
TNT:NNAP	TOZMUS	400.302	361.863	1.106	35.107	1.539	1.620	5.263
TNT:1-BN	URIJAH	434.201	359.316	1.208	28.743	1.737	1.777	2.303
TNT:DMDBT	URIKUC	431.363	421.063	1.044	24.216	1.496	1.524	1.872
TNT:PDA	URILAJ	341.275	310.756	1.079	31.515	1.578	1.578	0
TNT:DMB	URILEN	365.297	344.786	1.059	24.105	1.501	1.547	3.065

[a] M are in g mol^{-1}, V_m in Å^3, the $\upsilon\sigma_{tot}^2$ in (kcal mol)^2 and all the density units are in g cm^{-3}.

$$R^2 = 1 - \frac{\sum_i \left(y_{exp,i} - y_{pre,i}\right)^2}{\sum_i \left(y_{exp,i} - y_m\right)^2} \quad (20)$$

where the predicted value of the cocrystal density was abbreviated as y_{pre}. The corresponding experimental value of the cocrystal density was abbreviated as y_{exp}, the mean values of the experimental densities of all the cocrystals was abbreviated as y_m, and N represents the total number of the cocrystals.

3 Results and discussion

The training set was 42 randomly selected cocrystals, the test set was 9 randomly selected cocrystals, and the validation set was 9 randomly selected cocrystals in the ANN model. The dataset whose serial numbers ranged from 1 to 42 was taken as the training set. The dataset whose serial numbers ranged from 43 to 51 was taken as the test set. The dataset whose serial numbers ranged from 52 to 60 was taken as the validation set. The descriptors (ρ_1, ρ_2, ΔE_{hb}, Ms, RTm, and E1u) were taken as the input data and trained.

ρ_1 and ρ_2 are the experimental densities of the cocrystals from the Cambridge Structural Database. They are calculated according to the experimental crystal cell parameters or are directly determined by experimental measurements. ΔE_{hb} is the energy difference of the strongest hydrogen bond interactions. Ms, RTm, and E1u are the dragon descriptors, and they have been indicated that they have a relation to the density in the ref. 8. For the choice of the descriptor, one method is that the important descriptors are decided by the relative analysis from thousands of descriptors. The other method is that the important descriptor with the physical meaning is directly selected by the expert's experiences. In the present study, six parameters were selected mainly according to the ref. 8, 11 and 15. The ANN model was taken as Model-I. Table 2 lists the predicted density using the artificial neural network model (ρ_{ANN}), experimental density (ρ_{exp}), and relative percentage error (Re%) of the 60 organic cocrystals. From Table 2, it can be seen that the predicted densities agree well with the experimental densities for all the cocrystals in the research study. The maximum absolute value of Re% is 6.48%, and the smallest absolute value of Re% is 0%. 88.3% of the absolute value of Re% of all 60 cocrystals was less than 3%, and 8.3% was between 3 and 5, and 3.3% was more than 5. The RMSE, MAE, and R^2 of 60 cocrystal densities predicted by the ANN model were 0.033, 0.023, and 0.920, respectively. 88.3% of the total results had an error of less than 0.05 g cm^{-3}. The RMSE and MAE of 50 energetic cocrystals, according to the prediction results of the ref. 9 were 0.077 and 0.066. In order to compare, R^2 of 50 energetic cocrystals from the ref. 9 was also calculated according to eqn (20), and the value was 0.825. 40% of the total results had an error of less than 0.05 g cm^{-3}. The densities of 50 energetic cocrystals from the ref. 9 were predicted according to the method of the ref. 8, and the RMSE, MAE, and R^2 were 0.490, 0.413, and 0.023, respectively. 40% of the total results had an error of less than 0.05 g cm^{-3}. From the view of RMSE, MAE, R^2, and the error range, the ANN model in the present work has a better prediction performance.

In order to compare the prediction results of the two models, 42 cocrystals used in Model-I were also used as the training set in Model-II, and the rest were used for verification. The three parameters α, β, and γ in eqn (16) were obtained by the least-squares method.

The specific formula is as follows:

$$\rho = 1.1105218 \times \left(\frac{M}{V_m}\right) + 0.0005218 \times \left(\upsilon\sigma_{tot}^2\right) + 0.336077 \quad (21)$$

Table 5 Parameters and the predicted density of the 6 unoptimized cocrystals[a]

Co-formers	Ref. code	M	V_m	M/V_m	$\upsilon\sigma_{tot}^2$	ρ_{exp}	ρ_{pre}	Re%
CL-20:AZ2	TETTAQ	672.320	492.017	1.366	45.318	1.939	1.929	−0.516
TNT:NNAP	TOZMUS	400.302	349.462	1.145	37.773	1.539	1.574	2.274
TNT:1-BN	URIJAH	434.201	347.532	1.249	31.624	1.737	1.741	0.23
TNT:DMDBT	URIKUC	431.363	401.162	1.075	26.426	1.496	1.461	−2.34
TNT:PDA	URILAJ	341.275	299.556	1.139	43.138	1.578	1.564	−0.887
TNT:DMB	URILEN	365.297	328.383	1.112	26.551	1.501	1.521	1.332

[a] M are in g mol^{-1}, V_m in Å^3, $\upsilon\sigma_{tot}^2$ in (kcal mol)^2, and all the density units are in g cm^{-3}.

 © 2021 The Author(s). Published by the Royal Society of Chemistry

Open Access Article. Published on 24 March 2021. Downloaded on 11/15/2025 10:46:23 AM.
This article is licensed under a Creative Commons Attribution-NonCommercial 3.0 Unported Licence.

Table 6 Comparison of the prediction results of the two organic cocrystal density prediction models

No.	Co-formers	Ref. code	R_{ANN}%	R_p%	$\lvert R_{ANN}\%\rvert - \lvert R_P\%\rvert$
1	CL-20:TNT	IZUZUZ	0.994	−3.023	−2.029
2	CL-20:DNG	JABYOD	−0.052	3.464	−3.412
3	CL-20:MTNP	QAPNAZ	−0.425	−2.574	−2.149
4	CL-20:AZ2	TETTAQ	−0.660	−3.213	−2.553
5	CL-20:NEX-1	WEPGEG	0.461	0.837	−0.376
6	CL-20:GTA	XAQFUS	0.053	6.010	−5.957
7	CL-2:TODAAZ	HIVGAW	−0.266	−4.721	−4.455
8	CL-20:NFQN	ROSMIX	−0.176	2.155	−1.979
9	CL-20:BQN	ROSMOD	0	5.864	−5.864
10	CL-20:DNB	TIVJUF	0.442	−1.070	−0.628
11	CL-20:4,5-MDNI	NILCIX	0.554	−1.770	−1.216
12	HMX:PNO	WEPTAP	−0.902	−0.094	0.808
13	HMX:FA	ZEZHET	1.689	3.205	−1.516
14	HMX:PDCA	ZEZGOC	−2.245	4.164	−1.919
15	BTF:TNA	ZEVNUL	1.122	3.612	−2.49
16	BTF:TNB	GEXMED	1.600	0.940	0.66
17	BTF:MATNB	GEXMON	0.327	0.178	0.149
18	BTF:TNA	GEXMIH	−0.119	−3.414	−3.295
19	TNT:NNAP	TOZMUS	0.466	5.740	−5.274
20	TNT:1-BN	URIJAH	−0.314	0.151	0.163
21	TNT:Ant	URIJEL	1.121	3.305	−2.184
22	TNT:9-BN	URIJIP	−2.760	1.404	1.356
23	TNT:Per	URIJUB	0.243	0.616	−0.373
24	TNT:T2	URIKEM	3.425	−7.213	−3.788
25	TNT:DMDBT	URIKUC	−0.421	3.187	−2.766
26	TNT:PDA	URILAJ	0.426	2.882	−2.456
27	TNT:DMB	URILEN	−2.475	5.585	−3.11
28	TNT:TNB	NIBJUF	1.119	6.364	−5.245
29	ABA:TNT	URILUD	−0.057	2.632	−2.575
30	MACIC:TZM	ACERAD	0	1.027	−1.027
31	DHDS:TZM	ACETEJ	−0.542	2.555	−2.013
32	DNBZA:NA	AWUDEB	−1.724	1.648	0.076
33	MBD:MTNB	DIFZOK	−1.077	4.434	−3.357
34	PM:UREA	EFOZAB03	−1.229	−4.243	−3.014
35	MC:PC	FIXROV01	−0.169	0.470	−0.301
36	AB:MTNB	FONHOH	−1.780	4.618	−2.838
37	NDT:THTZT	FOYSUJ	−0.483	1.237	−0.754
38	IDT:NTZ	FUFSOQ	0.920	1.931	−1.011
39	DNBA:BA	GAUTAM15	0.560	−8.347	−7.787
40	PZ:OA	GUDSUV	0.915	−1.977	−1.062
41	TNP:MDNI	HARJOB	−0.061	−1.367	−1.306
42	DNBA:TA	IJAKAH	2.908	2.712	0.196
43	NMI:NMI	ITIXUE	−0.207	0.504	−0.297
44	AN:HP	JOZZED	−4.788	−2.151	2.637
45	NF:CA	LEWTAK	−6.483	2.634	3.849
46	NF:UREA	ORUXUV	1.846	1.673	0.173
47	NPO:PA	OWIYEZ	4.924	2.806	2.118
48	UREA:CA	PANVUV	1.223	0.477	0.746
49	PZCX:DHXBED	PAQNOM	−0.181	1.302	−1.121
50	DNPA:ODADA	QARQUY	2.045	−3.761	−1.716
51	TNP:TAD	QONYUP	−4.407	−1.930	2.477
52	IZO:DLTA	RUWPEG	1.143	−0.686	0.457
53	IZO:LTA	UHACIQ	1.718	−0.873	0.845
54	IZO:LTA	UHAFEP	1.772	1.420	0.352
55	DNBZA:TZ	UNAWUD	1.805	3.015	−1.21
56	Urea:OA	UROXAM	−1.077	0.707	0.37
57	PZCX:OA	UZODUK	0.793	−0.942	−0.149
58	TZA:NDTZI	VAZBIJ	3.983	−4.740	−0.757
59	TZTM:HP	YAFFUJ	1.413	−4.515	−3.102
60	BM:TNP	YUQHEY	−5.140	1.028	4.112

The predicted densities of the 60 cocrystals using the surface electrostatic potential correction model are presented in Table 3. Table 3 lists the predicted densities using the surface electrostatic potential correction model (ρ_P), experimental densities (ρ_{exp}), and relative percentage errors (Re%) of the 60 cocrystals. From Table 3, it can be seen that the predicted densities are also in good agreement with the experimental densities for all the cocrystals in the study. The maximum absolute value of Re% is 8.346%, and the smallest absolute value of Re% is 0.094%. In the 60 predicted results of the cocrystal densities, 60% of the absolute values of Re% was between 0 and 3, 28.3% was between 3 and 5, and 11.67% was greater than 5. The RMSE, MAE, and R^2 of 60 cocrystal densities predicted by the surface electrostatic potential correction model are 0.055, 0.045, and 0.716, respectively. 65.0% of the total results had an error of less than 0.05 g cm^{-3}. According to the ref. 17, for CHNO molecular crystals, the RMSE, MAE, and R^2 of 36 molecular crystals are 0.045, 0.036, and 0.918, respectively. 77.8% of the total results had an error of less than 0.05 g cm^{-3}. According to the ref. 18, an R^2 value greater than 0.5 indicates the significant predictivity of the model. In the ref. 17, Politzer *et al.* categorized the quality of the density predictions according to the criteria provided by Kim *et al.*,[18] that is, (a) "excellent" (having an error less than 0.03 g cm^{-3}), (b) "informative" (having an error between 0.03 and 0.05 g cm^{-3}), (c) "barely usable" (an error between 0.05 and 0.10 g cm^{-3}), and (d) "deceptive" (error greater than 0.10 g cm^{-3}). Compared to the pure energetic crystal, the prediction based on MESP exhibits worse performance. However, according to the ref. 17, Model-II was also acceptable.

While the Politzer model was built, the Politzer parameters were calculated based on the packing unit structure of the experimental crystal. However, in fact, while the model was used, the packing unit structure of the experimental crystal was not obtained, and it was only obtained by theoretical optimization. In order to compare the error caused by the packing unit structure, the densities of the six cocrystals were predicted based on the packing unit structures coming from the experimental cocrystals, which were theoretically optimized and unoptimized, respectively.

The specific calculated values are shown in Table 4 and 5, respectively. By comparing the predicted densities of the cocrystals based on the optimized and unoptimized packing unit structures, it could be found that the Re% of the predicted density values was comparable with that of the predicted density values based on the unoptimized cocrystals. Therefore, the Politzer model built in the present study can be used to predict the densities of the cocrystals.

In order to compare the relative accuracy of the artificial neural network model and the surface electrostatic potential correction model in predicting the cocrystal density, the differences between the absolute values of the Re% of the two models were calculated. Table 6 shows the values of R_{ANN}%, R_P%, and the differences between the absolute values of R_{ANN}% and R_P% ($\lvert R_{ANN}\%\rvert - \lvert R_P\%\rvert$). The regression performance of the two models for predicting the densities of the cocrystals is shown in Fig. 2. When the value of $\lvert R_{ANN}\%\rvert - \lvert R_P\%\rvert$ is negative, it indicates that the artificial neural network model is more accurate in predicting the density value of the cocrystal.

Open Access Article. Published on 24 March 2021. Downloaded on 11/15/2025 10:46:23 AM.
This article is licensed under a Creative Commons Attribution-NonCommercial 3.0 Unported Licence.

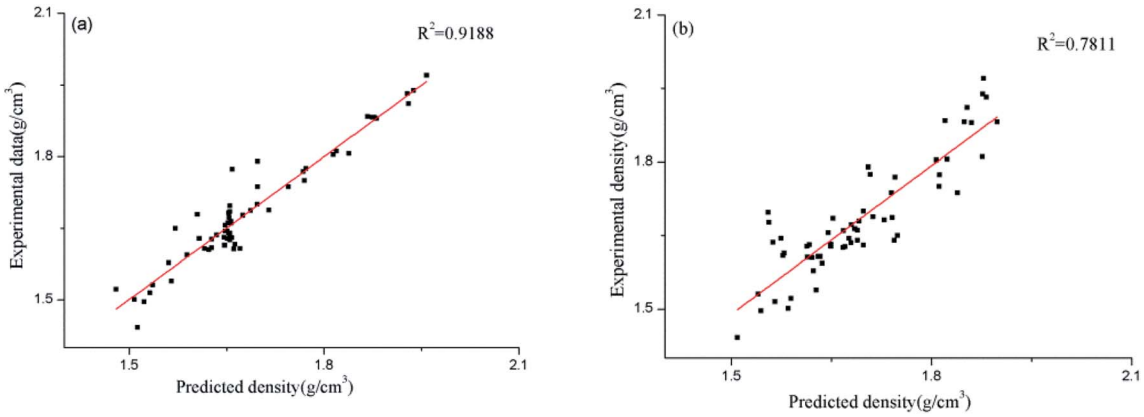

Fig. 2 Predicted densities of the cocrystals *vs.* experimental data for all the datasets ((a) for the ANN model, and (b) for the Politzer model).

However, the surface electrostatic potential correction model is more accurate in predicting the density value of the cocrystal. From Table 6, it can be seen that among the 60 cocrystals, 18 are positive values, accounting for 30%, and 42 are negative values, accounting for 70%. According to the RMSE and MAE values of the two models calculated above, it is also found that both values of the artificial neural network model are smaller than those obtained using the surface electrostatic potential correction model. From Fig. 2, it can also be seen that the performance of the artificial neural network model is better than that of the surface electrostatic potential correction model. Therefore, in these two models, the density value of the cocrystal predicted by the artificial neural network model is relatively accurate. However, the surface electrostatic potential correction model is more convenient to predict the cocrystal density because it provides a unique and specific formula for calculating the cocrystal density. It is also simple and time-saving to calculate the two parameters of the surface electrostatic potential correction model.

4 Conclusions

In this study, two types of prediction models for the organic cocrystal density were established. One is the artificial neural network model, and the other is the surface electrostatic potential correction model. For the artificial neural network model, the maximum absolute value of Re% is 6.483%, and the smallest absolute value of Re% is 0. 88.3% of 60 cocrystals for the absolute values of Re% were less than 3%. The RMSE and MAE of 60 organic cocrystal densities predicted by the artificial neural network model are 0.033 and 0.023, respectively. For the surface electrostatic potential correction model, maximum absolute value of Re% is 8.346%, and smallest absolute value of Re% is 0.094%. In the 60 predicted results of the cocrystal densities, 60% of the absolute values of Re% were between 0 and 3, 28.3% was between 3 and 5, and 11.67% was greater than 5. The RMSE and MAE of the 60 cocrystal densities predicted by the surface electrostatic potential correction model are 0.055 and 0.045, respectively.

To compare the prediction accuracy of the two models, the values of $|R_{ANN}\%| - |R_P\%|$ were also calculated. By comparing the values of Re%, RMSE, MAE, and $|R_{ANN}\%| - |R_P\%|$, it can be inferred that the artificial neural network model is more accurate than the surface electrostatic potential correction model. However, the surface electrostatic potential correction model is more convenient and practical than the artificial neural network model. Therefore, the two models could be selected according to the actual requirements.

Conflicts of interest

The authors declare there are no conflicts of interest regarding the publication of this paper.

Acknowledgements

The authors acknowledge the support of the National Natural Science Foundation of China (21805303).

Notes and references

1 Z. W. Yang, H. Z. Li, X. Q. Zhou, C. Y. Zhang, H. huang, J. S. Li and F. D. Nie, *Cryst. Growth Des.*, 2012, **12**, 5155–5158.
2 O. Bolton and A. J. Matzger, *Angew. Chem., Int. Ed.*, 2011, **50**, 8960–8963.
3 X. G. Xue, Y. Ma, Q. Zeng and C. Y. Zhang, *J. Phys. Chem. C*, 2017, **121**, 4899–4908.
4 H. B. Zhang, C. Y. Guo, X. C. Wang, J. J. Xu, X. He, Y. Liu, X. F. Liu, H. Huang and J. Sun, *Cryst. Growth Des.*, 2013, **13**(2), 679–687.
5 L. Kazandjian and J. F. Danel, *Propellants, Explos., Pyrotech.*, 2006, **31**, 20–24.
6 K. B. Landenberger and A. J. Matzger, *Cryst. Growth Des.*, 2010, **10**, 5341–5347.
7 C. Y. Zhang, Y. F. Cao, H. Z. Li, Y. Zhou, J. H. Zhou, T. Gao, H. B. Zhang, Z. W. Yang and G. Jiang, *CrystEngComm*, 2013, **15**, 4003–4014.
8 M. Fathollahi and H. Sajady, *Struct. Chem.*, 2018, **29**, 1119–1128.
9 Z. Narges and G. F. Mohammadkhani, *Cent. Eur. J. Energ. Mater.*, 2020, **17**(1), 31–48.

 © 2021 The Author(s). Published by the Royal Society of Chemistry

Open Access Article. Published on 24 March 2021. Downloaded on 11/15/2025 10:46:23 AM.
This article is licensed under a Creative Commons Attribution-NonCommercial 3.0 Unported Licence.

10 I. V. Tetko, J. Gasteiger, R. Todeschini, A. Mauri, D. Livingstone, P. Ertl, V. A. Palyulin, E. V. Radchenko, N. S. Zefirov, A. S. Makarenko, V. Y. Tanchuk and V. V. Prokopenko, Virtual computational chemistry laboratory – design and description, *J. Comput.-Aided Mol. Des.*, 2005, **19**, 453–463.
11 G. R. Krishna, U. Marko, Z. Jacek and Å. C. Rasmuson, *Cryst. Growth Des.*, 2018, **18**, 133–144.
12 P. Politzer, J. Martinez, J. S. Murray, M. C. Concha and A. Toro-labbé, *Mol. Phys.*, 2009, **107**, 2095–2101.
13 A. Nirwan, A. Devi and V. D. Ghule, *J. Mol. Model.*, 2018, **24**, 166.
14 D. Musumeci, C. A. Hunter, R. Prohens, S. Scuderi and J. F. McCabe, *Chem. Sci.*, 2011, **2**, 883.
15 J. H. Zhou, M. B. Chen, W. M. Chen, L. W. Shi, C. Y. Zhang and H. Z. Li, *J. Mol. Struct.*, 2014, **1072**, 179–186.
16 T. Lu and F. W. Chen, *J. Comput. Chem.*, 2012, **33**, 580–592.
17 P. Politzer, J. Martinez, J. S. Murray, M. C. Concha and A. Toro-Labbé, *Mol. Phys.*, 2009, **107**(19), 2095–2101.
18 C. K. Kim, S. G. Cho, C. K. Kim, H. Y. Park, H. Zhang and H. W. Lee, *J. Comput. Chem.*, 2008, **29**(11), 1818–1824.